IEEE Access
Multidisciplinary | Rapid Review | Open Access Journal

Received January 11, 2021, accepted February 20, 2021, date of publication February 23, 2021, date of current version March 5, 2021.

Digital Object Identifier 10.1109/ACCESS.2021.3061587

Concurrent Optimization of Mountain Railway Alignment and Station Locations With a Three-Dimensional Distance Transform Algorithm Incorporating a Perceptual Search Strategy

HAO PU[1,2], XIAOMING LI[1,2], PAUL M. SCHONFELD[3], WEI LI[1,2], JIAN ZHANG[4], (Member, IEEE), JIE WANG[5], JIANPING HU[6], AND XIANBAO PENG[7]

[1]School of Civil Engineering, Central South University, Changsha 410075, China
[2]National Engineering Laboratory for High Speed Railway Construction, Central South University, Changsha 410075, China
[3]Department of Civil and Environmental Engineering, University of Maryland, College Park, MD 20742, USA
[4]School of Computer Science and Engineering, Central South University, Changsha 410075, China
[5]China Railway First Survey and Design Institute Group Co., Ltd., Xi'an 710043, China
[6]China Railway Eryuan Engineering Group Co., Ltd., Chengdu 610031, China
[7]China Railway Siyuan Survey and Design Group Co., Ltd., Wuhan 430063, China

Corresponding author: Wei Li (leewei@csu.edu.cn)

This work was supported in part by the National Science Foundation of China (NSFC) under Grant 51778640 and Grant 51608543, in part by the Project of Science and Technology Research and Development Plan of China National Railway Group Co., Ltd., under Grant P2019G003, in part by the Hunan Province Open Foundation for University Innovation Platform under Grant 20K140, in part by the High-Speed Railway Infrastructure Joint Fund of the National Natural Science Foundation of China under Grant U1734208, and in part by the Key Laboratory of Roads and Railway Engineering Safety Control, Shijiazhuang Tiedao University, Ministry of Education, under Grant STKF201901.

ABSTRACT The design of railway alignment and station locations involves two intertwined problems, which makes it a complex and time-consuming task. Especially in mountainous regions, the large 3-dimensional (3D) search spaces, complex terrain conditions, coupling constraints and infinite numbers of potential alternatives of this problem pose many challenges. However, most current optimization methods emphasize either alignment optimization or station locations optimization independently. Only a few methods consider coordinated optimization of alignment and stations, but optimize them sequentially. This paper proposes a concurrent optimization method based on a 3-dimensional distance transform algorithm (3D-DT) to solve this problem. It includes the following components: (1) To optimize the location of stations within specified spacing intervals, a novel perceptual search strategy is proposed and incorporated into the basic 3D-DT optimization process. (2) A combined-alignment-station 3D search neighboring mask is developed and employed to search for both the alignment and stations. In order to implement the perceptual process, two additional kinds of 3D reverse perceptual neighboring masks are also developed and employed in the algorithm. (3) Multiple coupling constraints between alignment and stations are also formulated and addressed during the search process. In this study, the effectiveness of the method is verified through a real-world case study in a complex mountainous region. The optimization results show that the proposed method can find high-quality alternatives satisfying multiple coupling constraints.

INDEX TERMS Railway, alignment, station location, concurrent optimization, mountainous areas, distance transform.

I. INTRODUCTION

The design of rail alignments and the location of stations are two intertwined issues arising in the strategic planning stage of rail investment. Usually, the goal of railway location optimization is to find the most economical alternative for railway alignment and station locations between two specified points [1]. To this end, designers usually start from a broad area and then narrow the search space to several possible corridors before finally focusing on the detailed location

The associate editor coordinating the review of this manuscript and approving it for publication was Bijoy Chand Chatterjee.

designs in the selected corridor. This process consumes much time. Besides, due to the requirements of designing railway alignment and station location concurrently, the design process is also restricted by the intricate interactions among them. For example, each station should be entirely located on a tangent section in a relatively flat area; the station should be located within the appropriate station spacing interval; overlapping stations with tunnels or bridges should be avoided. These interactions are represented with various coupling constraints, which should be handled during the concurrent optimization process. Thus, optimizing railway alignment and station locations concurrently in mountainous areas is a complex and time-consuming process.

However, although this issue has long been of interest in the scientific literature, most methods still optimize the alignment and stations separately, with most studies focusing on the alignments. Since the 1960s, many researchers have invested substantial efforts into automated alignment optimization. These alignment optimization methods are normally classified into two groups, namely direct and indirect methods.

In direct approaches, an alignment can be defined by a series of points of intersection (PIs) that are connected sequentially. The optimization model is formulated by treating the PIs' coordinates and radii as variables and computing them directly. Direct methods include calculus of variations [2], [3], numerical search [4], [5], linear programming [6], enumeration [7], particle swarm optimization [8]–[10], and genetic algorithms [11]–[15]. In indirect approaches, the methods first generate an optimized path or corridor before finally deriving from them the PIs' coordinates and radii. Indirect methods include network optimization [16], dynamic programming [17], [18], mixed integer programming [19], discrete algorithms [20], and distance transform [21]–[26]. Detailed discussions of these methods can be found in our earlier publications [22], [23]. It is worth noting that all of the above direct or indirect methods have focused on optimizing the alignment between two or more predetermined stations.

In recent years, the distance transform (DT) has drawn our attention for alignment optimization problems in complex mountainous regions. Compared with flat plain regions, the terrain fluctuates drastically in mountainous regions. High mountains and deep valleys fill the landscape, in which bridges and tunnels are the major constructions. Thus, railway alignment optimization in these regions is more difficult than in flatter regions. The distance transform (DT) has great potential in solving this problem. DT was originally designed for image processing [27], and was first applied to railway and road alignment design satisfying a gradient constraint by De Smith [21]. This algorithm provided a effective method for generating the alignment between two end points, by approximating the global distances through propagating local distances within an $n \times n$ adjacency matrix with rectangular $S_X \times S_Y$ cells which is called the neighboring mask (Fig. 1). The value in each cell of the neighboring mask

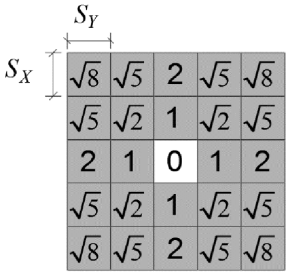

FIGURE 1. A 2D 5 × 5 neighboring mask.

is the local distance from that cell to the central cell. Then Li *et al.* [22] developed an improved bidirectional distance transform for railway alignment optimization in complex mountainous regions. In further developments, Li *et al.* [23] set cutting planes for horizontal points of intersection (HPIs) on the angle bisectors at the key points of the paths generated by DT and then searched for an optimized solution using an improved genetic algorithm (GA). Pu *et al.* [25] developed a 3-dimensional distance transform (3D-DT) by using an erythrocyte-shaped 3D neighboring mask and a stepwise-backstepping strategy that greatly increase the feasible search spaces. This method can find more alignment alternatives with higher qualities. However, these methods cannot be used for the concurrent optimization of an alignment and stations along it.

Researchers have also attempted to optimize station locations. The first known paper dealing with the location of railway stations from an optimization perspective was published over 100 years ago by Müller. Other early papers on the subject were summarized and extended in a prominent paper by Vuchic and Newell [28], who developed an optimization model to determine the interstation spacing for minimizing the travel time on rail transit lines. Vuchic [29] improved that model by also considering passenger demand in finding the station locations which maximize ridership. Wirasinghe [30], [31] formulated a mathematical model of a coordinated rail and bus transit system. Chien and Schonfeld [32] also developed a model for jointly optimizing the characteristics of a rail transit route and its feeder bus network. Laporte, Mesa and Ortega [33] developed a model for locating a fixed number of stations along a railway line so that the demand covered by the stations would be maximized. An improved version of this work can be found in Laporte, Mesa and Ortega [34], and extended to bus station location by Gleason [35], Murray [36], [37], Wu and Murray [38]. Other significant contributions to the railway station location problem were provided by [39]–[43]. They all sought to balance the tradeoffs between minimizing the number of stations and maximizing demand coverage, in order to comprehensively consider the positive and negative effects of placing an additional station in an existing railway alignment. Besides, Lovett *et al.* [44] developed a model using station, route, and system data to evaluate the stations and routes by maximizing a profit objective function, and found the factors which

have greatest impact on the costs and returns of alignments. However, the above methods can address only station location optimization issues when the railway alignments are known.

In addition, a few studies did consider alignment and stations optimization at the same time, but ignored the coupling constraints and interactions among them. Instead, they generated several stations first and then optimized the alignment connecting those stations. Such methods involved bi-criterion mathematical programming [45], tabu search [46], two-phase heuristic algorithms [47], and genetic algorithms (GA) [14]. Besides, some commercial software and applications focus on generating a multitude of low-cost alignment options, while treating a station separately as an obligatory point or another independent start and end point during the optimization process, overlooking the coupling characteristics between alignment and stations such as station spacing constraints. Therefore, the above methods cannot optimize the stations and alignment concurrently.

It is worth mentioning that in recent studies, researchers have begun to focus on concurrent optimization of alignment and stations while considering the coupling constraints. Lai and Schonfeld [15] first presented a concurrent railway station location and alignment optimization methodology. The methodology first constructs the candidate pool of potential rail transit stations based on the consideration of various site requirements regarding topological features, accessibility to the existing roadway network and land availability. These candidates are then selected along with generating the alignment between each pair of neighboring stations, using the embedded GA-based heuristic concurrent optimization model to minimize the total system cost while satisfying station selection and track geometry constraints. From a local perspective, the alignment is still generated after searching through stations although some coupling constraints are considered. The alignment can only pass through locations of candidate stations. A better station location may be found but probably by compromising the location of the alignment. Thus, the final combined solution may not be optimized.

In an extended effort, Pu *et al.* [24] also developed an optimization model for concurrently optimizing railway alignment and station locations considering railway costs and multiple constraints, and proposed a DT (two dimensional)-based backtracking search algorithm to generate the stations while searching the railway alignment. This method can be applied for more general terrains, including complex mountainous regions. Nevertheless, this method is also imperfect. The proposed backtracking search strategy first selects local connection paths that satisfy the constraints of station spacing, then moves the station's center along this selected path, and finally obtains the feasible station location. Therefore, the search space of the station is limited to the area covered by the local path. A better alignment location may be found but probably by compromising the location of the station. Therefore, the final combined solution may also not be the optimized.

As shown above, although various studies have focused on optimizing alignments and station locations, none has really solved the problem of optimizing railway alignment and station locations concurrently. Instead, they adopted the idea of completely or partially separating the alignment and stations to solve the problem of concurrent optimization, which forced either the alignment or the station to accommodate the other. For instance: a) With a pre-determined station location: The alignment must pass through the pre-set station locations so that the search space of the alignment is restricted. Various promising alignments are ignored and the final alternative may not be good enough. b) With a pre-determined global/local alignment: The station can only be located on the alignment and this method neglects many promising station locations. The optimized combination of stations and alignment cannot be found with the above methods. Thus, it is preferable to optimize the alignment and station concurrently.

To this end, we propose a concurrent optimization method based on a 3-dimensional distance transform algorithm. As noted above, the 3-dimensional distance transform algorithm has significant advantages in terms of alignment optimization: it can consider the linkages of two cells above or below the ground surface and can find more alternatives with higher qualities. However, it is not usable for optimizing the alignment and stations concurrently. Thus, unlike the basic 3-dimensional distance transform algorithm, this study focuses on the following aspects:

(1) The concurrent optimization means that both the alignment and stations are searched simultaneously. However, the station should only be searched and set in a specified interval along the rail line. With the classic distance transformation algorithm, the first searched station location can easily be regarded as the optimum, ignoring other better locations that may generated in subsequent searches. Thus, in order to find the best alternative within the interval, the perceptual search strategy is proposed and incorporated into the basic search algorithm to perceive the promising station alternatives in subsequent searches.

(2) In order to satisfy the requirements of concurrent optimization, a combined-alignment-station 3D search neighboring mask is developed and employed in the search process along with the basic alignment search mask [25]. Besides, two other kinds of 3D reverse perceptual neighboring masks are also developed and employed in the perceptual search process. In general, four neighboring masks are employed in the optimization process, two of which are used in the search process and two others are used in the perceptual process.

(3) Moreover, multiple complex constraints, including terrain, geometric, structure and location constraints about the alignment and stations, are handled during the search process.

The remainder of this paper is organized as follows. In the ''Optimization Model'' section, an optimization model is formulated for the concurrent optimization problem of railway alignment and station locations. In the ''Concurrent 3D-DT Search Algorithm'' section, a combined-alignment-station

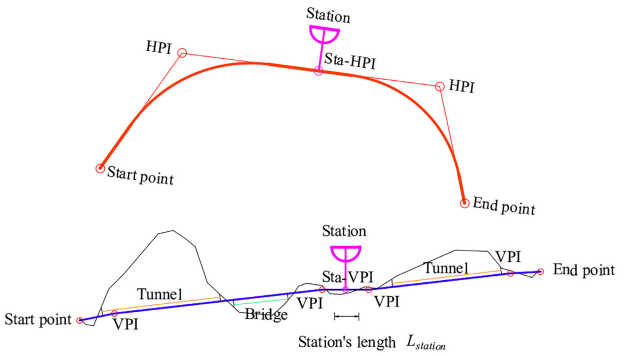

FIGURE 2. A 3D railway alignment with a station.

3D search neighboring mask, two kinds of the reverse 3D perceptual neighboring masks, and the 3DDT-based concurrent optimization algorithm incorporating a perceptual search strategy are proposed to solve the formulated optimization model. In the ''Case Study'' section, a detailed description of a real-world case study is provided to demonstrate the effectiveness of the proposed method. Finally, in the ''Conclusions'' section, the paper's conclusions and recommendations for further studies are presented.

II. OPTIMIZATION MODEL

The concurrent optimization problem of railway alignment and station locations is to find the most economical railway alignment and station locations between two specified points based on topography, soil conditions, and environmental impacts, while satisfying multiple constraints, such as on railway design specifications, forbidden zones, and coupling constraints among railway alignment and station locations. Besides, the large continuous search space, complex constraints and infinite numbers of potential alternatives to this problem pose many challenges. Hence, an effective 3-dimensional optimization model is desirable. In the model, an alignment can be defined by a series of points of intersection (PIs) that are connected sequentially [8], [12]. Points of intersection include horizontal points of intersection (HPIs) and vertical points of intersection (VPIs). Station locations can also be expressed by Sta-HPIs and Sta-VPIs, as shown in Fig. 2.

The optimization model used here has the general form of our previous model [24]. It can be summarized in terms of four aspects: comprehensive geographic information model (CGIM, [22]), design variables, objective function and multiple constraints. A detailed description is presented below.

A. COMPREHENSIVE GEOGRAPHIC INFORMATION MODEL (CGIM)

The comprehensive geographic information model is used to store and manage the essential information for railway alignment and station design, such as topography, satellite images, ground objects, soil conditions, forbidden areas, unit costs and some major technical standards. The data structure of the model is a rectangular lattice. This model provides the foundation information of the distance transform (DT) algorithm as well as the 3-dimensional distance transform (3D-DT) algorithm. A more detailed description can be found in our previous studies [24], [26].

B. DECISION VARIABLES

(1) Alignment: since a 3D railway alignment can be determined by its HPIs and VPIs, the data on HPIs and VPIs are used as design variables for the 3D railway alignment optimization problem. Conventionally, the HPIs' data include the coordinates X_i, Y_i, horizontal curve radius R_i and transition curve length l_{Ti}. The VPIs' data include the mileage K_i, design elevation H_i and vertical radius R_{Vi}. However, the l_{Ti} are not treated as design variables, since l_{Ti} can be obtained directly when the R_i is determined in China (Code for Design of Railway Line, China Ministry of Railways, 2017). Moreover, the vertical curve radius R_{Vi} is also not treated as design variable since it is a fixed value determined by the railway grade in China (Code for Design of Railway Line, China Ministry of Railways, 2017). It should be noted that although they are not treated as design variables, both transition curve and vertical curves are considered during the optimizing process. Therefore, the basic alignment optimization problem is reduced to finding the vector set of **X, Y, R, K, H** for a 3D alignment.

(2) Station: the station locations can also be determined by the horizontal data Sta-HPIs and the vertical data Sta-VPIs. The Sta-HPIs include the coordinates of station center (X_{si}, Y_{si}); the Sta-VPIs include the mileage K_{si} and the design elevation H_{si}. However, the station must be on the alignment. Hence, if the mileage K_{si} of the station is determined, the coordinates of the station center (X_{si}, Y_{si}) can also be determined easily. Therefore, the basic station optimization problem is reduced to finding the vector set of $\mathbf{K_S}$, $\mathbf{H_S}$.

C. OBJECTIVE FUNCTION

The objective function used in this model is the total cost of the alignment and stations, which includes railway alignment-related costs (C_{ali}), station-related costs (C_{sta}) and operational costs (C_{op}):

$$F(X, Y, R, K, H, K_S, H_S) = \Delta(C_{ali} + C_{sta}) + C_{op} \quad (1)$$

$$\Delta = i(1+i)^n/[(1+i)^n - 1] \quad (2)$$

$$C_{ali} = C_e + C_l + C_t + C_b + C_{ra} \quad (3)$$

$$C_{sta} = C_s + C_{rs} + C_f \quad (4)$$

$$C_{op} = C_{ang} + C_{len} + C_{gra} \quad (5)$$

where Δ is the capital recovery factor, which converts the total construction costs to uniform construction costs per year; i is the interest rate (% per year) and n is the number of compounding periods (economic life). Railway alignment-related costs (C_{ali}) include the earthwork cost (C_e), length-related construction cost (C_l), tunnel construction cost (C_t), bridge construction cost (C_b) and right-of-way cost

(C_{ra}). Station-related costs (C_{sta}) include station construction cost (C_s), right-of-way cost of the station (C_{rs}) and station facility cost (C_f). Operational costs (C_{op}) include the operating cost sensitive to horizontal turning angle (C_{ang}), alignment length (C_{len}) and gradient (C_{gra}).

Detailed formulations for computing the objective function can be found in our previous publication [24], [25].

D. MULTIPLE CONSTRAINTS

The multiple constraints in the concurrent optimization model can be classified as alignment constrains and coupling constraints. The alignment constraints are presented in detail in our previous publication [48], [25]. They include three types: geometric constraints, structure constraints and location constraints:

i: Geometric constraints: (1) the minimum radius of the horizontal circular curves (R_{min}); (2) the minimum length of the horizontal circular curves (L_{Cmin}); (3) the minimum length of tangent between two adjacent horizontal curves (L_{Tmin}); (4) the maximum gradient of vertical slope sections (G_{max}); (5) the minimum length of vertical slope sections (L_{Smin}); (6) the maximum absolute difference between adjacent gradients (ΔG_{max}).

ii: Structure constraints: (1) the maximum bridge height (H_{Bmax}); (2) the maximum tunnel length (L_{Tmax}); (3) the minimum gradient in tunnels (G_{Tmin}) should be also constrained, for drainage; (4) the station's length ($L_{station}$); (5) the minimum and maximum spacing ($D_{sta-min}$, and $D_{sta-max}$) between adjacent stations.

iii. Location constraints: (1) The alignment and stations should not be set in forbidden zones. (2) The crossing constraints should be checked to insure that the clearance (H_c) is sufficient when an alignment crosses the existing rivers, transportation infrastructure (roads, railways) and utilities.

The proposed model and approach focus on finding the optimized combination of station locations and alignment, as well as handling the coupling constraints between them. In the model, a station is treated as a rectangular area defined by its length (L_{sta}) and width (W_{sta}), which contains railway tracks, equipment for operation and maintenance of the station, the pre-set curves and other components. The length of the station area (L_{sta}) consists of the station's length ($L_{station}$) and the pre-set length of the horizontal and vertical curves. The width of the station area (W_{sta}) is specified by designers according to China's Code for Design of Railway Lines (CDRL, China Ministry of Railways, 2017).

In this section, we concentrate on presenting the coupling constraints for alignments and stations, which can be classified into horizontal constraints and vertical constraints.

1) THE HORIZONTAL CONSTRAINTS

The station locations must satisfy both horizontal and vertical constraints along the alignment. The horizontal constraints are used to locate stations on feasible horizontal locations along the alignment. They consist of station spacing constraints and geometric constraints.

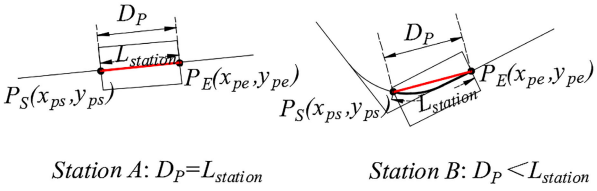

FIGURE 3. Geometric constraints of alignment and station.

(1) Station spacing constraints between adjacent stations

According to traffic capacity and operation safety demands, the station distribution should satisfy the station spacing constraint:

$$D_s \in [D_{sta-\min}, D_{sta-\max}] \tag{6}$$

where D_s is the spacing between two adjacent stations (km), $D_{sta-min}$ is the minimum spacing required between adjacent stations (km), and $D_{sta-max}$ is the maximum spacing allowed between adjacent stations (km).

(2) Geometric constraints of alignment and station

The stations should be located in a tangent section, for operational safety. Assuming that P_S and P_E are the two ends of a station on the alignment (see Fig. 3), the horizontal alignment within the station should satisfy (7).

$$D_P = [(x_{Ps} - x_{Pe})^2 + (y_{Ps} - y_{Pe})^2]^{0.5} = L_{station} \tag{7}$$

where D_P is the actual distance from P_S to P_E along the alignment (m), $L_{station}$ is the station's length, x_{Ps}, y_{Ps} are the coordinates of P_S (m), and x_{Pe}, y_{Pe} are the coordinates of P_E (m).

If $D_P < L_{station}$, then the station is set on a curve (see station B in Fig. 3); if $D_P = L_{station}$ then the station is set on the tangent section. (See station A in Fig. 3.)

2) THE VERTICAL CONSTRAINTS

The vertical coupling constraints are used to locate stations on the feasible vertical locations along the alignment. They consist of gradient, station-tunnel and station-bridge constraints.

(1) Gradient constraints within the station

The station should be set on a relatively flat area to prevent trains from sliding. Therefore, the maximum average gradient (i_{smax}) of the link path containing the station should be smaller than the maximum design gradient (i_{max} or G_{max}). For example, for two cells ($C_{i,j}$ and $C_{m,n}$) in Fig. 4, the maximum gradient (i_{smax}) between them is computed with (10), rather than with the maximum design gradient (i_{max} or G_{max}) according to the design specification. The gradient (i_g) between them must satisfy (8) to ensure that the local path still satisfies the gradient constraint after a relatively flat station area is located.

$$i_g \le i_{s\max} \tag{8}$$

$$i_g = h/l_s \tag{9}$$

$$i_{s\max} = (l_s \times i_{\max} - h_s)/l_s \tag{10}$$

$$\Delta h = \left|H_{i,j} - H_{m,n}\right| \tag{11}$$

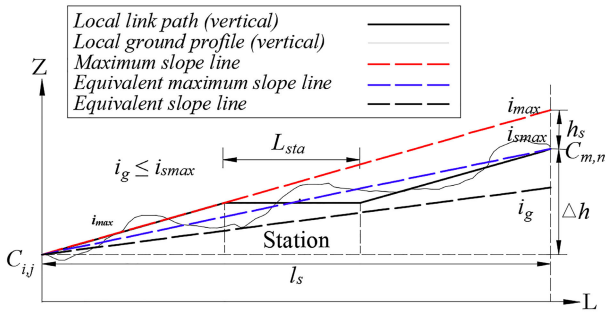

FIGURE 4. Gradient constraint within the station.

$$l_s = \sqrt{\left(x_{i,j} - x_{m,n}\right)^2 + \left(y_{i,j} - y_{m,n}\right)^2} \tag{12}$$

$$h_s = i_{\max} \times L_{sta} \tag{13}$$

In (8 – 13) i_g is the gradient between two linked cells (‰), i_{smax} is the maximum average gradient (i_{smax}) of the link path containing the station (‰), Δh is the ground elevation difference of the cell located at row m and column n in the lattice (m), $H_{i,j}$ is the elevation of the cell located at row i, column j in the lattice (m), $H_{m,n}$ is the elevation of the cell located at row m, column n in the lattice (m), $x_{i,j}$, $y_{i,j}$ are the coordinates of the cell located at row i and column j in the lattice (m), $x_{m,n}$, $y_{m,n}$ are the coordinates of the cell located at row m and column n in the lattice (m), h_s is the lost elevation due to the relatively flat station area (m) and L_{sta} is the length of the station area (m).

(2) Station-tunnel and station-bridge constraints

Setting a station in a tunnel or a bridge significantly increases the construction investment and difficulty of construction and maintenance. Therefore, overlapping the station location with tunnels and bridges should be avoided. We assume that the ground elevation of a random cell located at row i and column j is $H_{Gi,j}$ and the design elevation of the station is H_S. The station-tunnel and station-bridge constraints can be expressed as follows:

(1) station-tunnel constraints (when $H_S < H_{Gi,j}$):

$$H_{Gi,j} - H_S < H_T \tag{14}$$

(2) station-bridge constraints (when $H_S > H_{Gi,j}$):

$$H_S - H_{Gi,j} < H_B \tag{15}$$

where H_T is the threshold depth (m) beyond which a tunnel is preferred to a deep cut, and H_B is the threshold height (m) beyond which a bridge is preferred to a fill.

III. CONCURRENT 3D-DT SEARCH ALGORITHM FOR ALIGNMENT AND STATION LOCATIONS

A. THE 3-DIMENSIONAL DISTANCE TRANSFORM ALGORITHM (3D-DT)

Two-dimensional distance transform (2D-DT) algorithms [21], [22] provide effective methods for generating the alignment between two target points, by approximating the global distances through propagating local distances within the neighboring mask. The distance propagating mechanism is embodied in (16).

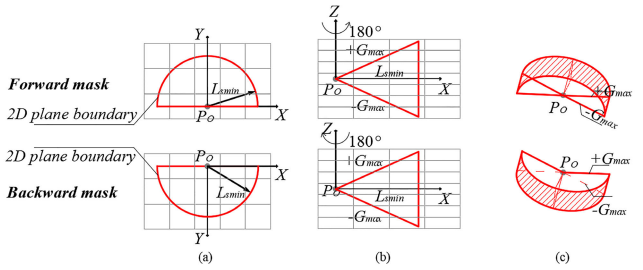

FIGURE 5. The generation process for 3D neighboring mask.

When cell p is scanned:

$$D^t(p) = D^{t-1}(q) + d\left[\Delta R\left(p\right), \Delta C\left(p\right)\right] \tag{16}$$

$$\Delta R(p) = r(q) - r(p) \tag{17}$$

$$\Delta C(p) = c(q) - c(p) \tag{18}$$

where $D^t(p)$ and $D^{t-1}(q)$ are the minimum distance from the cell p or cell q to the target cell, $d\left[\Delta R\left(p\right), \Delta C\left(p\right)\right]$ is the minimum distance from cell p to cell q, $\Delta R(p)$ and $\Delta C(p)$ are the incremental row and column movements from cell p to cell q. This distance propagation process takes place within the neighboring cells, which are called the neighboring mask. The neighboring mask used in 2D-DT is described in detail in De Smith [21] and Li *et al* [23]. In the theory of 3D-DT, the basic idea remains the same, and the relation between a 2D "cell" and a 3D "voxel" is defined as follows [25]: in 3D digital images, each cell on X-Y plane corresponds to a set of vertical voxels at the same plane location in the 3D space. For the railway alignment optimization problem, the voxel dimensions are anisotropic: the sizes of two planar dimensions are generally the same; however, the size in the Z-direction is much smaller than the two planar sizes ($S_X = S_Y \gg S_Z$).

Besides, an erythrocyte-shaped 3D neighboring mask (Fig. 5c) is developed. Its design steps are as follows: (1) Take a random cell's central point (P_O) as the center and the minimum length of vertical slope sections (L_{smin}) as the radius to form a semicircular boundary on the X-Y plane (Fig. 5a). (2) Take P_O as the origin and the ± maximum gradient ($\pm G_{max}$) as two slopes, respectively, forming a closed triangle on the X-Z plane (Fig. 5b). (3) Rotate the triangle by 180° around the Z-axis on P_O and obtain the final mask (Fig. 5c).

The basic search flow of 3D-DT can be summarized as follows: (1) The distance of each voxel in the lattice is initialized: the value of the destination is zero (0) and the others are infinity (∞). (2) A two-pass scan of the lattice data is conducted: a forward scan from the top left to the bottom right and a backward scan from the bottom right to the top left. When one voxel is scanned, the center of the neighboring mask is placed over it and the local distance is propagated step by step. (3) The above process is repeated until no value of voxels changes and different alternatives are generated.

The detailed explanation of the above method can be found in our previous publication [25].

B. CONCURRENT 3D-DT SEARCH ALGORITHM FOR ALIGNMENT AND STATION LOCATIONS

As mentioned earlier, the concurrent search algorithm should generate the alignment and stations at the same time, which means the search simultaneity should be reflected in the algorithm. Otherwise, whichever is determined first, the other is restricted by the coupling constraints. To satisfy this requirement, a combined-alignment-station 3D search neighboring mask and the 3D reverse perceptual neighboring masks are specified. Meanwhile, a new perceptual search strategy is also proposed and incorporated into the basic 3D-DT algorithm in order to solve this problem better. The details are presented below.

1) THE COMBINED-ALIGNMENT-STATION 3D SEARCH NEIGHBORING MASK

The basic erythrocyte-shaped 3D neighboring mask should be modified to be able to search for both alignment and stations. Therefore, we specify a combined-alignment-station neighboring mask by combining the erythrocyte-shaped 3D neighboring mask and station to search for both. According to China's Code for Design of Railway Lines (China Ministry of Railways, 2017), the station must be set on a relatively flat area. The station location is abstracted into a flat section, and added into the original neighboring mask. The length of this flat section corresponds to the length of station area (L_{sta}), The scale of the combined mask is extended to account for the station addition. Thus, the step length ($L_{smin-step}$) should be the sum of the length of station area (L_{sta}) and the minimum length of vertical slope sections (L_{smin}). It can be computed exactly with (19).

$$L_{s\min-step} = L_{sta} + L_{s\min} \tag{19}$$

In addition, the horizontal scale of the combined neighboring mask is expanded, but the height stays unchanged. Thus, the maximum comprehensive gradient (G_i) of the mask also changes. It can be computed exactly with (20).

$$G_i = (i_{\max} \times L_{s\min})/L_{s\min-step} \tag{20}$$

Therefore, we can obtain the combined-alignment-station3D search neighboring mask through the following steps:

(1) Take a random cell's central point (P_O) as the center and the step length ($L_{smin-step}$) as the radius to form a semicircular boundary on the X-Y plane (Fig. 6a).

(2) Take P_O as the origin and take the maximum comprehensive gradient ($\pm G_i$) as two slopes forming a closed frame on the X-Z plane (Fig. 6b).

(3) Rotate the triangle by 180° around the Z-axis on P_O and obtain the final mask (Fig. 6c).

In the search process, we only scan the voxels located on the 3D circular boundary (the dashed area in Fig. 6c). It is

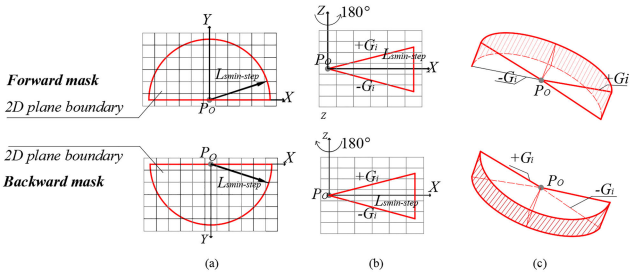

FIGURE 6. Generation process of the combined-alignment-station 3D search neighboring mask.

because (1) the voxels located within the 2D plane boundary (Fig. 6a) cannot satisfy the minimum length constraint for vertical slope sections (L_{smin}) and the length constraint for station area (L_{sta}); (2) voxels located on the 2D plane boundary but above the upper curved surface or below the lower curved surface of the mask cannot satisfy the G_i constraint. This combined neighboring mask can be used to search and locate both the alignment and station simultaneously. The combined-alignment-station 3D search neighboring mask is similar in shape to the erythrocyte-shaped search neighboring mask. However, its comprehensive gradient decreases and its longitudinal scale widens. It may be called a flattened erythrocyte-shaped 3D neighboring mask. Still, there are significant differences in the usage of these two masks. When any voxel of the basic erythrocyte-shaped 3D neighboring mask is scanned during the search process, the local link path can be generated by connecting this voxel to the central voxel directly. The local comprehensive cost can be computed exactly based on this local connection path. However, the connection method in the combined-alignment-station 3D search neighboring mask is more complicated.

For instance, for any central voxel V_c, the voxel V_t within the combined-alignment-station 3D search mask is scanned. The local path connected from V_c to V_t must accommodate the flat area of the station, while satisfying the minimum slope length constraint (L_{smin}). There are only two connection methods, as shown in Fig. 7: a) Station front: The station is set at the front of the mask, and then connected to a minimum slope section. b) Station rear: The station is set at the rear of the mask and is connected after the minimum slope section. Both of these local paths are considered, and two local comprehensive costs ($Dist_a$ and $Dist_b$) are obtained correspondingly. The local path with lower local comprehensive cost is used as the final path connecting V_c to V_t. By analogy, when all voxels in the mask are scanned, the best local path with the minimum cost is recorded in the central voxel V_c.

However, since concurrent optimization of alignment and stations is the problem to be solved, it is infeasible to just use the combined 3D neighboring mask to search, because the local link path obtained by the combined neighboring mask must be with a station, as shown in Fig. 7. The final scheme violates constraints such as that on station spacing ([$D_{sta-min}$, $D_{sta-max}$]). Therefore, there are two application requirements for the combined 3D neighboring mask: 1) It must be

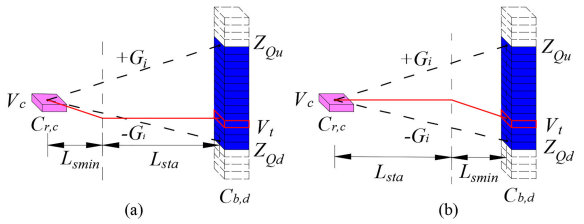

FIGURE 7. Two connection methods in the combined-alignment-station 3D search neighboring mask: a) Station front; b) Station rear.

applied within a confined station spacing interval [$D_{sta-min}$, $D_{sta-max}$] for the station spacing constrains. 2) Even more importantly, the combined 3D neighboring mask must be used along with the basic erythrocyte-shaped 3D neighboring mask (which is called the alignment 3D search neighboring mask in the following passages), in order to form a standard alignment. Although the alignment 3D neighboring mask and the combined-alignment-station 3D search neighboring mask are different in scale and search scope (both planar and longitudinal, as shown in Fig. 5 and Fig.6), they can still be applied together as follows: When one voxel is scanned in the search process, the center of this two neighboring masks is placed over it in order of first the alignment 3D search neighboring mask and then the combined-alignment-station 3D search neighboring mask. After scanning the voxels in the search area of these two masks separately, if at least one voxel exists which satisfies the constraints for each mask, each local distance ($Dist_{sta}$ obtained by the combined-alignment-station 3D search neighboring mask and $Dist_{ali}$ obtained by the alignment 3D search neighboring mask) is added to the value of the central voxel. These new values ($Dist_{sta}$ and $Dist_{ali}$) are the minima of all the searched voxels set in each neighborhood mask. Finally, all 3-dimensional incremental movements are also recorded and two local link paths are generated from the central voxel to the searched voxels.

2) THE 3D REVERSE PERCEPTUAL NEIGHBORING MASK

In most cases, by placing the above two search neighboring masks at any central voxel, it is easy to find the local optimized link path in each neighboring mask and obtain two distance values accordingly. However, in order to find the optimized alignment and station alternative, it is even more critical to make a good decision on two local link paths.

For the concurrent optimization of alignment and station proposed in this study, it is emphasized that the alignment and station should be searched simultaneously. Thus, the first found station may easily be regarded as the best station in the specified interval, due to the unknown pros and cons in subsequent searches. This case is called "the locally optimal dilemma", as shown in Fig. 8, which leads to an inadequate alignment-station combined result.

A 3DDT-based search algorithm incorporating a perceptual search strategy and two kinds of reverse 3D perceptual neighboring masks are proposed to find the potential link paths in subsequent searches. The perceptual result provides a reference for choosing the better one between the link paths with and without a station. This section focuses on the description of the reverse 3D perceptual neighboring mask while the perceptual strategy will be described in detail in later sections. Because the perceptual mask is used to find the potential link paths in subsequent searches and scan the un-scanned voxels, it is oriented in the opposite direction from the search mask. Thus, we will find that the perceptual mask is just the reverse search mask. Besides, the perceptual mask is also divided into the combined-alignment-station 3D perceptual neighboring mask and the alignment 3D perceptual neighboring mask. The search masks and perceptual masks during the two-pass scan are shown in Fig. 9.

Although the perceptual mask is almost the same as the search mask except for its direction, the scanning process is somewhat different. The combined-alignment-station 3D perceptual neighboring mask must also be used together with the alignment 3D perceptual neighboring mask: when one voxel is scanned in the perceptual process, the centers of these two perceptual neighboring masks are placed over this central voxel (first the alignment 3D perceptual neighboring mask and then the combined-alignment-station 3D perceptual neighboring mask). All voxels in the search area of the two masks will be scanned, and if there exists one voxel satisfying all constraints in each mask, it is connected downward from the central voxel. Two kinds of local distance ($Dist_{per-sta}$ obtained by the combined-alignment-station 3D perceptual neighboring mask, and $Dist_{per-ali}$ obtained by the alignment 3D perceptual neighboring mask) will be added to each connected voxel, rather than the central voxel (Fig. 10). In addition, it is emphasized that, in the next step, the mask will be placed on each connected voxel to continue to scan the un-scanned voxel downwards.

3) THE 3DDT-BASED CONCURRENT OPTIMIZATION ALGORITHM INCORPORATING THE PERCEPTUAL SEARCH STRATEGY

As noted earlier, a combined-alignment-station 3D search neighboring mask or an alignment search neighboring mask can only find and connect the lowest-cost voxel within the mask and then find a locally optimal path step by step. However, such a locally optimal result is obtained by considering a narrow circular scanning area coverage (Fig. 5c and Fig. 6c), but ignoring the effect and feedback between the current connection decision and the subsequent searches, which is crucial for the concurrent optimization. It has slight impact on the alignment search process, but great impact on the stations location selection: According to the basic flow of 3D-DT, the first found station may easily be regarded as the optimal station, forming a non-optimal alignment and station combination result. This case is also called "the locally optimal dilemma", as shown in Fig. 8. Thus, for the concurrent optimization of alignment and stations, it is necessary to ensure that the final alignment and stations avoid the locally optimal

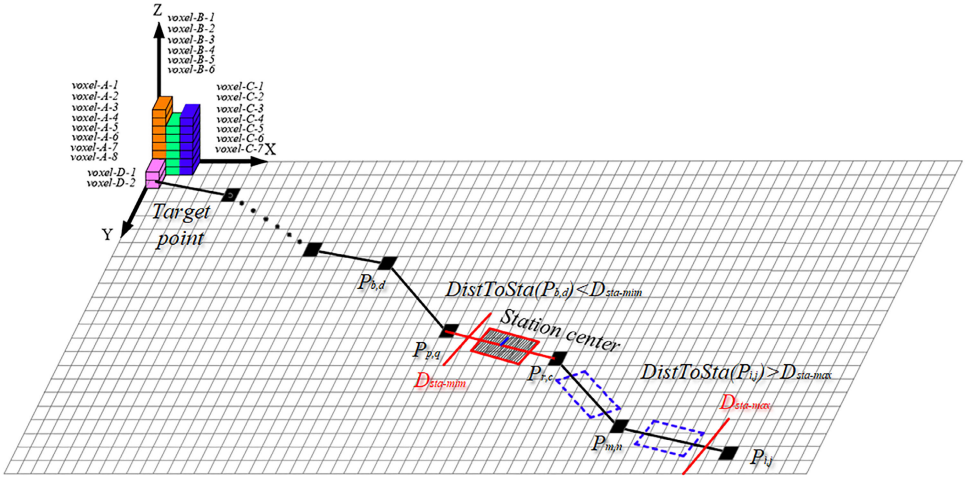

FIGURE 8. The locally optimal dilemma in search process: the solid rectangle is the first found provisionally optimal station and the dashed rectangle is the potential optimal station in subsequent searches.

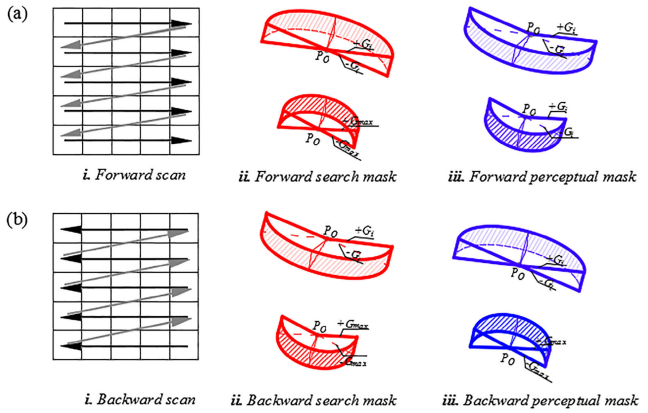

FIGURE 9. Two kinds of search masks and perceptual masks during the two-pass scan.

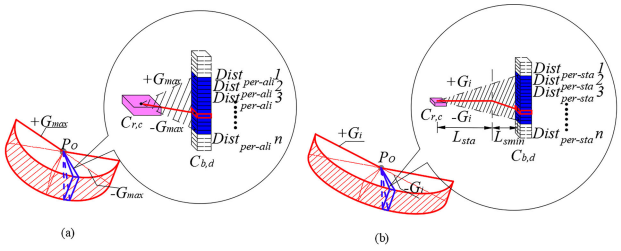

FIGURE 10. Two kinds of perceptual masks used in the perceptual process and two kinds of local distance ($Dist_{per-sta}$ obtained by the combined-alignment-station 3D perceptual neighboring mask and $Dist_{per-ali}$ obtained by the alignment 3D perceptual neighboring mask) are added to each connected voxel.

dilemma. Therefore, the 3DDT-based concurrent optimization algorithm incorporating the perceptual search strategy is proposed to find the potential link paths in subsequent searches and provide feedback for the current connection decision. The perceptual search process is as follows:

(1) Station spacing check

Before the detailed description of the search process, the station spacing update mechanisms in the search process and perceptual process are introduced.

1) In the search process

During the search process, the neighboring mask is placed on the central voxel. After the best link voxel within the mask is found, station spacing of the central voxel is computed and recorded simultaneously. We create a station spacing attribute *DistToSta* for all voxels in three dimensions to store the distance value from the current cell to the nearest generated station in the previous search process. This attribute is used to determine when to start searching for the station locations using the combined mask. Assuming that $p_{i,j}$ is the current cell, $p_{m,n}$ is one of the cells in its neighboring mask. After finding the best link cell, the *DistToSta* ($p_{i,j}$) value is renewed with (21) as shown in Fig. 11.

$$DistToSta(p_{i,j}) = DistToSta(p_{m,n}) + D_{i,j} \tag{21}$$

where $p_{m,n}$ is the best-linked cell, and $D_{i,j}$ is the distance from cell $p_{i,j}$ to cell $p_{m,n}$ (m).

2) In the perceiving process

If $DistToSta\ (p_{m,n}) \geq D_{sta-min}$, then a station-search process and a perceptual process is conducted step-by-step (as described in the following section), until one cell $p_{f,g}$ exceeds the constraint of $D_{sta-max}$. Especially, due to different usage methods of the perceptual mask, the station spacing attribute is renewed with (22) as shown in Fig. 12:

$$DistToSta(p_{r,c}) = DistToSta(p_{i,j}) + D_{per-i,j} \tag{22}$$

where $p_{r,c}$ is the best connected cell in the perceptual mask, and $D_{per-i,j}$ is the distance from cell $p_{i,j}$ to cell $p_{r,c}$ (m) obtained with the perceptual process.

(2) Basic search process:

The search process can be divided into three stages: the searching stage, the perceiving stage and the decision-making stage.

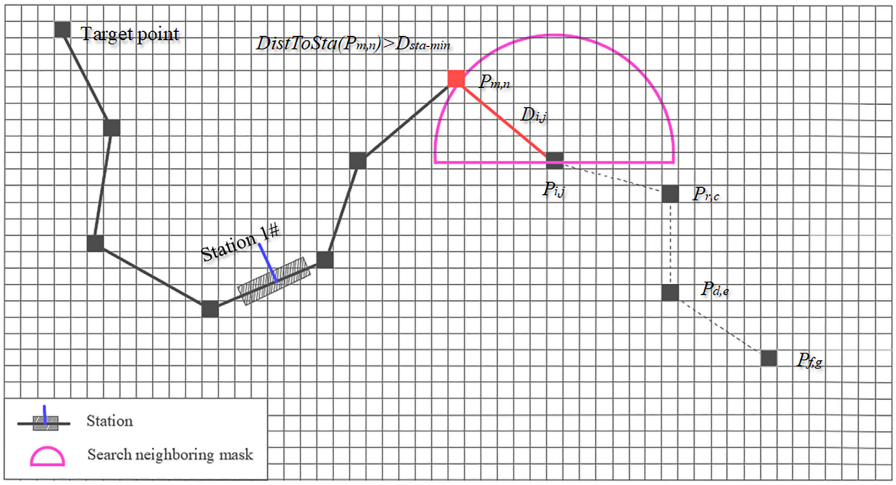

FIGURE 11. The station spacing update mechanism in the search process (X-Y plane).

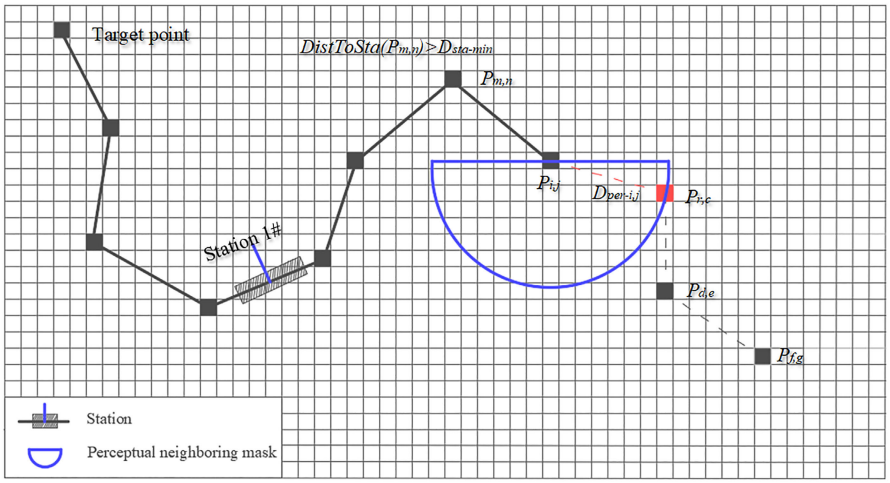

FIGURE 12. The station spacing update mechanism in the perceptual process (X-Y plane).

Stage 1: The searching stage:

Step 1: Initialize the distance of each voxel in the 3D digital image. The value of the destination voxel is zero (0), and the others are infinite (∞).

Step 2: Conduct a two-pass scan on X-Y plane by checking each ''cell'' across the image: a forward scan from the top left to the bottom right, and then a backward scan from the bottom right to the top left. After one cell is checked, we scan vertically all the voxels corresponding to that cell from top to bottom.

Step 3: When one voxel ($p_{p,q}$) is scanned, the center of the alignment search neighboring mask is placed over it and then the local distance (D_{ali}) is added to the value of the voxel. The new value of this voxel is the minimum of all the sums. Meanwhile, the distance value ($DistToSta_{ali}$ ($p_{p,q}$)) from the current cell to the nearest generated station in the previous search process is also recorded in the central voxel.

Step 4: Check the station spacing for the first time: If $DistToSta_{ali}$ ($p_{p,q}$) $\geq D_{sta-min}$, then a station-search process is conducted; go to step 5; otherwise, a station cannot be set on the local path; return to step 3 to scan the next adjacent voxel.

Step 5: The center of the combined-alignment-station 3D search neighboring mask is placed over the same voxel. The gradient constraints, crossing constraints, station-bridge constraints, forbidden area constraints (Fig. 13) and alignment-related constraints (described in [25]) are checked while scanning the voxels in the mask's circular area. If there exists at least one voxel that satisfies all the above constraints, then the other local distance (D_{sta}) is added to the value of the voxel, which is the minimum of all the sums. Besides, because the scales of the two above masks are different, the link path is also different, as shown in Fig. 14. Thus, another distance value ($DistToSta_{sta}(p_{p,q})$) from the current

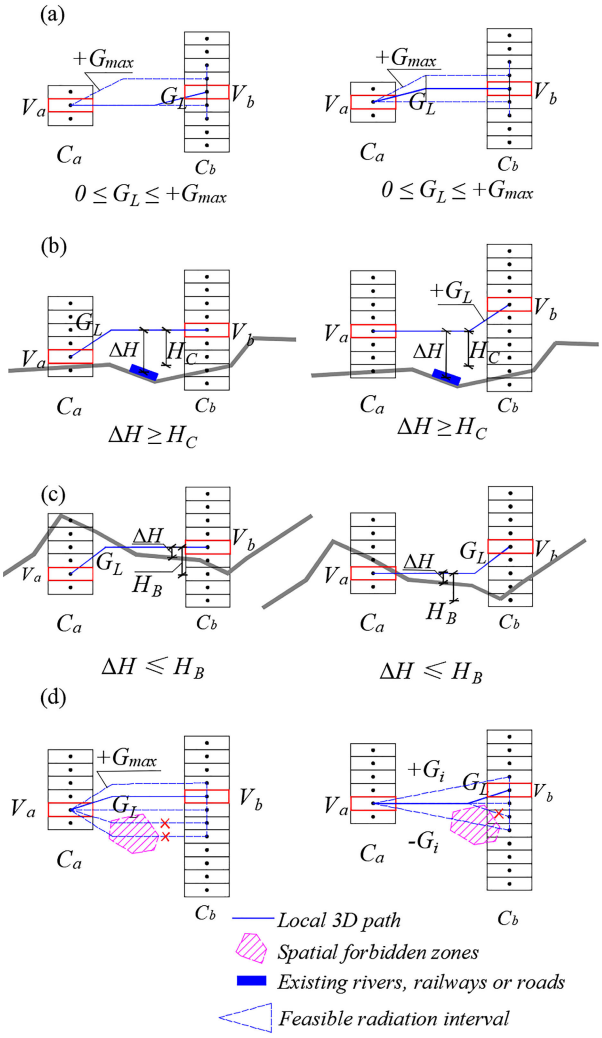

FIGURE 13. Station-related constraints when linking two voxels: (a) Gradient constraints; (b) Crossing constraints; (c) Station-bridge constraints; (d) Forbidden area constraints.

voxel to the nearest generated station is also renewed, and recorded for the central voxel.

Step 6: Check the station spacing constraint a second time, because two different neighborhood masks used here lead to the different connection paths. If $DistToSta_{sta}(p_{p,q}) \geq D_{sta-min}$, then go to step 7 for the perceiving phase (the second phase); otherwise, a station cannot be set on the local path, then return to step 3 to scan the next adjacent voxel.

Stage 2: The perceiving stage:

Perceive the potential link paths based on the two link paths generated by the above steps.

Step 7: The center of the alignment 3D perceptual neighboring mask, and the combined-alignment-station 3D perceptual neighboring mask are placed on the central voxel respectively, in order to scan voxels within each circular area following the scanning method described in previous section, while checking the slope constraints, forbidden area constraints, station-tunnel constraints, stations-bridge constraints, and alignment-related constraints.

Moreover, as the perceptual search process is affected by complex terrain and coupling constraints, its results can be divided into the following four cases, as shown in Fig. 15:

Case 1: Both alignment and station search results (V_{ali}, and V_{sta}).

Case 2: Only alignment search results (V_{ali}), and no station search results (V_{sta}).

Case 3: Only the station search result (V_{sta}), and no alignment search results (V_{ali}).

Case 4: Neither alignment nor station search results (no V_{ali}, and V_{sta}).

For the first three cases, renew and record each accumulated distance value (D_{ali}) and station distance value (*DistToSta*). Then go to step 8 to check station spacing constraints. For case 4, go to step 10 directly and enter the decision-making phase.

Step 8: Check the station spacing constraint for the third time. If $DistToSta \leq D_{sta-max}$ in each direction, go to step 9 and place the masks again to perceive downward; if $DistToSta \geq D_{sta-max}$ in each direction, then go to step 10 and enter the decision-making-stage.

Step 9: According to the following rules, place the centers of the two perceptual masks on the connected voxel searched in step 7: If the whole local path generated from step 3 to step 7 has no station, both the alignment 3D perceptual neighboring mask and the combined-alignment-station 3D perceptual neighboring mask are placed on the next voxel; otherwise, only the alignment 3D perceptual neighboring mask is placed. The specific situation is discussed as follows:

For case 1: Place both the alignment 3D perceptual neighboring mask and the combined-alignment-station 3D perceptual neighboring mask on the alignment search result (V_{ali}), and place only the alignment 3D perceptual neighboring mask on the station search result (V_{sta}).

For case 2: Place both the alignment 3D perceptual neighboring mask and the combined-alignment-station 3D perceptual neighboring mask on the alignment search result (V_{ali}).

For case 3: Place only the alignment 3D perceptual neighboring mask on the station search result (V_{sta}).

After that go to step 7 and continue to scan within the circular area of masks to update and record the accumulated distance values (D_{ali}, and D_{sta}) and station distance values (*DistToSta*) in each direction.

Stage3: The decision-making stage:

Step 10: According to the perceptual results, compare all local paths with and without a station obtained by previous steps and then choose the current best voxel. For example, for random central voxel V_c there are two link choices, V_{sta}, and V_{ali}, which are generated by step 5-6. Then, the perceptual process is conducted n times until reaching the maximum station spacing. If every perceptual step is successful, there will be $n+1$ generated paths, as shown in Fig. 17. Every local path corresponds to one comprehensive distance value, *Dist (1), Dist (2), Dist (3), . . ., Dist* $(n+1)$, which is recorded in the final voxel. Finally, choose the best link after comparing these $n+1$ distance values: 1) If any comprehensive distance

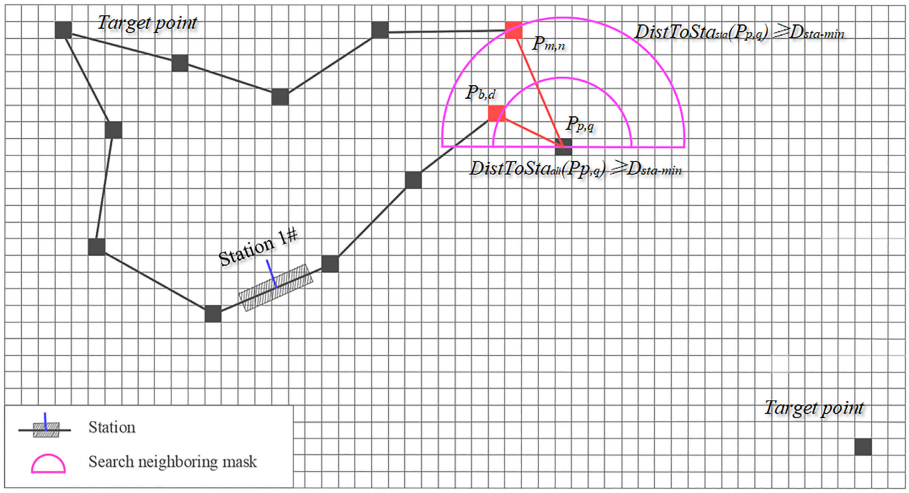

FIGURE 14. The search process using both the combined-alignment-station 3D search neighboring mask and the alignment search neighboring mask.

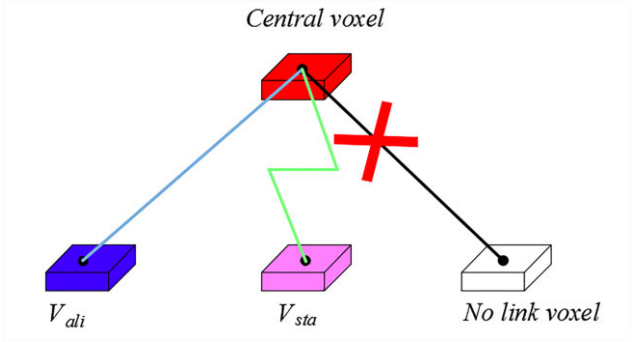

FIGURE 15. The link result of the central voxel: V_{ali} corresponds to the local path without a station; V_{sta} corresponds to the local path with a station.

value from *Dist1* to *Dist* (n) is below *Dist* $(n+1)$, the best link voxel of central voxel V_c is the V_{ali}. 2) Otherwise, only if all comprehensive distance values from *Dist1* to *Dist* (n) exceed *Dist* $(n+1)$, the best link voxel to the central voxel V_c is the V_{sta}.

Step 11: Repeat Steps 2-10 until no voxel value changes. The final value of every voxel is the minimum distance to the destination voxel. With these values the corresponding shortest path can be generated. Since there is only one zero-value (i.e. the destination point) on the distance map, we can always find a neighbor with a smaller Euclidean distance from any starting voxel if the voxel is not the destination. Therefore, the best path from an arbitrary source to the destination point is guaranteed to be found.

C. FITTING PROCESS

Because the generated alternatives are piecewise-linear polylines rather than smooth curves that satisfy the requirements of railway alignment design, these alternatives must be refined. The fitting process includes initializing and optimizing the generated alternatives as shown in Fig. 18. First, we select a series of horizontal and vertical key points in the polyline path as the points of intersection to generate the initial refined alternative (Fig. 18a). Next, a particle swarm optimization (PSO) based method [9] is employed to optimize the polylines in order to obtain the final alternatives, using the coordinates, elevations and projection mileage as input variables (Fig. 18b). During this process, a reduction of maximum gradient is considered. When trains run on horizontal curves ($R_s \cap R_c \neq \emptyset$, where R_s is the mileage range of every slope section while R_c is the mileage range of horizontal curves) or in tunnels ($\Delta H > H_T$, where ΔH is the elevation difference between the slope section and the ground surface while H_T is the threshold depth (m) favoring a tunnel rather than a deep cut), the additional resistance increases the difficulties of overcoming the maximum gradient. Therefore, the maximum gradient of the slope section in tunnels and curves must be reduced:

(1) The maximum gradient on curves is reduced through following equations:

$$i = i_{\max} - \Delta i_R \tag{23}$$

$$\Delta i_R = \frac{10.5\alpha}{L_i} \tag{24}$$

where $i_{\max}$ is the maximum gradient (‰), Δi_R is the reduced gradient on curves (‰), i is the maximum gradient on curves (‰), α is the horizontal turning angle (°), and L_i is the slope length (m).

(2) The maximum gradient in tunnels is also reduced through following equation:

$$i = i_{\max} - \Delta i_s = \beta_s \times i_{\max} \tag{25}$$

where $i_{\max}$ is the maximum gradient (‰), Δi_s is the reduced gradient in tunnels (‰), and β_s is the gradient reduction factor, which can be obtained according to China's Code for Design of Railway Line (CDRL, China Ministry of Railways,

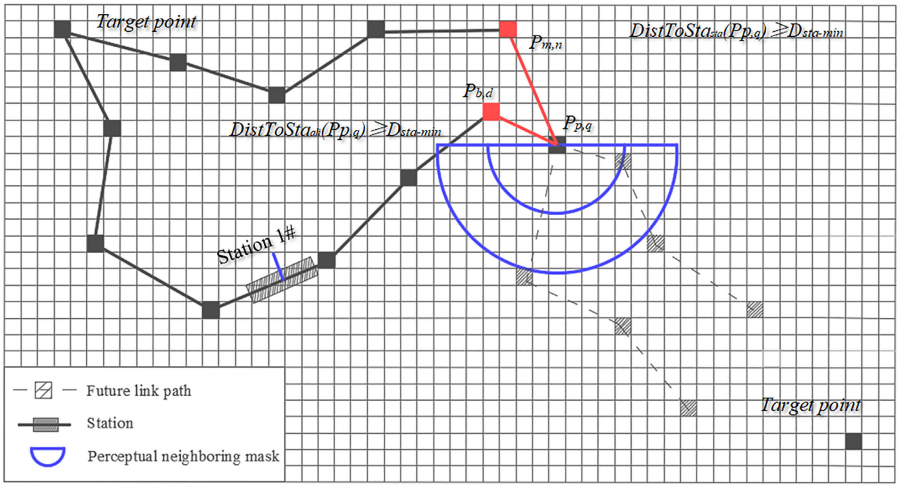

FIGURE 16. The perceptual process using both the combined-alignment-station 3D perceptual neighboring mask and the alignment perceptual neighboring mask.

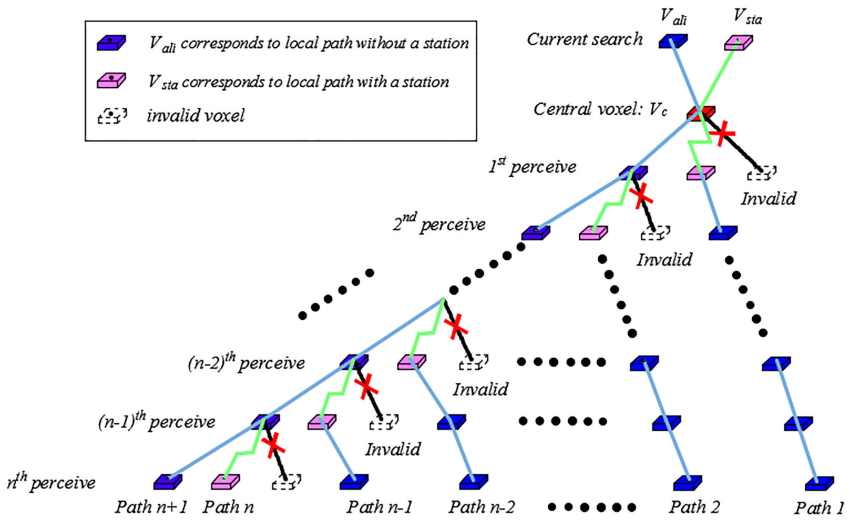

FIGURE 17. The local path tree obtained with the perceptual process.

2017). It is worth noting that (25) is also considered during the 3DDT-based search process.

This study focuses on the 3DDT-based search process. More detailed information on the fitting process and PSO method can be found in our earlier publication [9], [25].

IV. CASE STUDY

We applied the developed method to the railway from Dananshan to Jianzha, which is one section of the Xining-Chengdu railway which was actually constructed and used. Besides, the alternative obtained by an experienced human designer and the alternative generated with 2D-DT-based method proposed in our earlier publication [24] are also presented in this section for comparisons.

(1) Comparison with the method of optimizing or designing the alignment after station locations:

TABLE 1. Corresponding Relation Between Topographic Map Scale and CGIM Resolution.

Scale	Resolution/m	Scale	Resolution/m
1:100000	100/50	1:50000	50/25
1: 2000	2.5	1: 1000	2.5

The manual alternative is produced by experienced designers in the China Railway First Survey and Design Institute Group Co. Ltd. The designers first determine the station locations and then choose a feasible alignment to connect stations, forming the final combined scheme. This is a commonly used design process. However, because the alignment must pass through the pre-set station locations, many promising alignments are ignored.

(2) Comparison with the method of optimizing station locations after alignment:

TABLE 2. The Design Parameters.

A. CONSTRAINT PARAMETERS		
Geometric constraints	Minimum radius of curve (R_{min})	3,500m
	Maximum gradient (i_{max})	25‰
	Minimum length of tangent between horizontal curves (L_{Tmin})	120m
	Minimum length of horizontal circular curve (L_{Cmin})	120m
Station siting constraints	Minimum station spacing ($D_{sta\text{-}min}$)	15km
	Maximum station spacing ($D_{sta\text{-}max}$)	40km
B. STRUCTURE PARAMETERS		
Stations	Length of the station area(L_{Sta})	1400m
	Width of the station area (W_{sta})	400m
Bridges and Tunnels	Threshold depth to auto-set a tunnel (H_T)	20m
	Threshold height to auto-set a bridge (H_B)	15m

C. COST PARAMETERS

Item	Cost	Item	Cost
Rail track (¥/m)	4,000	One abutment (¥)	200,000
Right-of-way (¥/m^2)	72.3	(L≥10000m) Tunnel (¥/m)	83,200
Filling earthwork (¥/m^3)	18	(L≥1000m) Tunnel (¥/m)	71,200
Cutting earthwork (¥/m^3)	24	(L≥500m) Tunnel (¥/m)	55,400
(H<50) Bridge (¥/m)	32,300	(L<500m) Tunnel (¥/m)	39,200
(H≥50, L<500) Bridge (¥/m)	37,800	One tunnel portal (¥)	250,000
(H≥50, L≥500) Bridge (¥/m)	45,200		

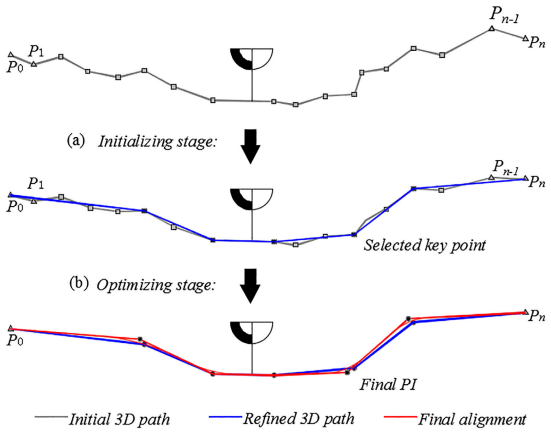

FIGURE 18. Refining an initial path into a final alignment.

The 2DDT-based method [24] adopts the backtracking search strategy, which means first selecting local connection paths that satisfy the station spacing constraints, then moving the station's center along this selected path, and finally obtaining the feasible station location. With this method, stations can only be located on the given alignment and many promising station locations are neglected.

A. RAILWAY PROJECT PROFILE

The Xining-Chengdu railway is a Grade I railway whose design speed is 200 km/h. It is located in the transitional zone between the Qinghai-Tibet Plateau, the Loess Plateau and the Western Sichuan Plateau. It crosses the two major river basins of the Yellow River and the Yangtze River. The terrain from Dananshan to Jianzha is especially undulating severely and characterized by high mountains, deep valleys, and many hills. The alignment must cross the watershed ridges of the Huangshui River and Yellow River. The terrain rises quickly from 2,150m to 4,400m within a distance of 40km, and then drops to 2070m within a distance of about 35km, which causes great difficulties in determining the alignment and station locations.

The study area is 4,482 sq. kilometers (54km × 83km). We represent this area using square lattices, in which 1,800 × 2,767 square cells in the X-Y plane are included, and the width of every cell is 30 m. At the same time, and quite unlike in 2D-DT, the voxels in the Z direction are also fully considered. The topography is shown in Fig. 19. The design parameters, including the constraint parameters, structure parameters and cost parameters, are shown in Table 2.

The cell's width corresponds to the resolution of the CGIM, which influences the accuracy of the computation results (e.g. right-of-way areas, filling and excavation earthwork): as CGIM's resolution increases, the accuracy of computation results also increases. In the area-corridor phase, designers usually work at a topographic map scale of 1:50000 or 1:100000. In the corridor-alignment phase, designers usually work at a topographic map scale of 1:2000 or 1:1000. According to the Quality Requirement for Digital Surveying

TABLE 3. Checks of Coupling Constraints.

Coupling constraints	Preference value	Manual alternative		Computer-generated alternatives (based on 2D-DT)		Computer-generated alternatives (based on 3D-DT)	
		Actual value	Check	Actual value	Check	Actual value	Check
1.Maximum spacing between two adjacent stations	≤40,000m	39,300m	√	33,998m	√	32,151m	√
2.Minimum spacing between two adjacent stations	≥15000m	17,750m	√	15,540m	√	20,630m	√
3.Gradient constraint within the station	Flat area	Flat area	√	Flat area	√	Flat area	√
4.Horizontal alignment constraint within the station	Tangent section	Partially-Curve section	√	Tangent section	√	Tangent section	√
5.Forbidden zones	Bypassed	Bypassed	√	Bypassed	√	Bypassed	√
6.Station-tunnel constraint	Non-overlapping	Non-overlapping	√	Non-overlapping	√	Non-overlapping	√
7.Station-bridge constraint	Non-overlapping	Partial-overlapping	√	Non-overlapping	√	Non-overlapping	√

TABLE 4. Comparison of the Best Alignments Obtained by an Experienced Human Designer, the 2DDT-Based Method, and the Proposed 3DDT-Based Method.

Item	Manual work	The lowest-cost alignment generated with the 2D-DT-based method	The lowest-cost alignment generated with the 3D-DT-based method
Length/m	79,700	78,213	79,900
Right-of-way/m^2	1,435,382	1,487,893	1,507,893
Embankment volume/m^3	1,392,464	1,024,938	576,377
Excavated volume/m^3	6,185,597	648,963	3,767,235
(H<50m) Bridge/Number-m	4-6,177.60	7-13,571.33	3-8,557.68
(H≥50, L<500m) Bridge/Number-m	2-794.12	1-502.21	/
(H≥50, L≥500m) Bridge/Number-m	23-14,597.15	12-8,772.87	9-13,112.37
(L≥10000m) Tunnel/Number-m	1-28,269.63	1-26,704.10	2-28,387.34
(L≥1000m) Tunnel/Number-m	9-27,457.38	8-21,526.87	6-14,935.03
(L≥500m) Tunnel/Number-m	1-885.67	4-2,815.37	3-2,214.43
(L<500m) Tunnel/Number-m	3-701.86	4-1,164.25	/
Alignment-related costs / million ¥	5779.01	5342.828502	4,897.927
Station-related costs / million ¥	121.30	107.45	76.86
Operation costs / million ¥	1,539.42	1,503.21	1,480.86
Total construction cost / million ¥	7,439.73	6,953.49	6,455.64
Total construction cost saving / million ¥	/	486.24	984.08
Percentage saving of comprehensive cost	/	6.54%	13.23%

and Mapping Achievements (State Bureau of Surveying and Mapping of China, 2008), different topographic map scales correspond to different CGIM resolutions:

Thus, at the first stage (the 3DDT-based search process), we usually recommend the establishment of a CGIM covering the whole research area with a resolution between 25m and 100m. Some experiments about the effect of cell widths have been presented in our previous publication [26]. The conclusions drawn from those experiments are that reductions in cell widths increase the computation results' accuracy, the quality of alternatives and the number of generated paths. For this case, the data we can download only provides 30m resolution, which is acceptable, so a 30 m x 30 m cell is selected in our study.

B. OPTIMIZATION RESULTS

The program runs on the HP Z600 workstation (Intel Xeon E5506 2.13 G processor, 4 GB RAM, 500 GB hard disk). The elapsed time of the optimization process is 6 h 54 m 38 s and seventy alternatives are generated. Because the station locations are also searched during the alignment search process, more computation time is needed than for alignment optimization in order to perceive the potential local paths in subsequent searches and handle the coupling constraints for the railway alignment and station locations. However, the computation time for this method is still acceptable because a skilled engineer would require more time to manually design even one feasible alternative for such complex conditions.

As shown in Fig. 19, two stations are generated with the above methods. The ability of all alternatives to satisfy the coupling constraints for railway alignment and station locations is verified in Table 3. The computer-generated stations are set at locations which satisfy both horizontal and vertical constraints, such as being within the given station spacing interval, in relatively flat areas, and not overlapping with forbidden areas, tunnels and bridges. However, one station in the manual alignment is not entirely on a tangent section. With limited time and resources, designers are unable to analyze all feasible solutions while handling such complex terrain conditions and design requirements. Therefore, the manual work cannot ensure that stations are located on tangent sections while not overlapping with the bridges and tunnels.

Compared with the manual one, the best alignment generated with the method presented in this paper is only 200m longer, as shown in Table 4, which is acceptable. Even more importantly, the tunnel lengths are reduced by a total of 11,777m while the bridge lengths are increased by only 101m, which means the construction cost is reduced significantly. As shown in Table 4, the comprehensive cost of manual work is 13.73% above the best alternatives generated with the proposed 3D-DT based method.

The comprehensive cost of the best alternatives generated with the 2DDT-based method is 6.54% below the manual alignment since the total length and the numbers of tunnels and bridges are reduced. However, its cost is still (6,953.49-6,455.647) / 6,953.49=7.16% above the best one generated with the proposed 3DDT-based method, because it still requires several extremely high bridges and long tunnels. Moreover, the station-related costs of the alternative generated with the 2DDT-based method are also (107.45-76.86) / 107.45=28.64% above the proposed 3DDT-based method, because the station can only be set along the given backtracking path, overlooking many promising locations. Due to the limited time and resources of human designers, the station-related costs of manual work are (121.30-107.45)/ 121.30=11.42% above the proposed 3DDT-based method and (121.30-76.86)/ 121.30=36.64% above the proposed 3DDT-based method. The detailed comparison results are presented in Table 4. In general, the 3DDT-based concurrent optimization method can generate a solution whose comprehensive cost is below the alternative obtained by an experienced human designer and generated with the 2DDT-based method.

It is worth mentioning that even experienced railway designers can only design one alternative at a time that satisfies all constraints, but the proposed method can offer 70 potential feasible alternatives in this case, which also exceeds the number of alternatives obtained by the 2DDT-based method (42 alternatives). In addition to the lowest-cost alternative, other alternatives also have their advantages and can provide some guidance to designers, who can compare them with the manual alternative to assess the improvement. To summarize, a 3DDT-based concurrent

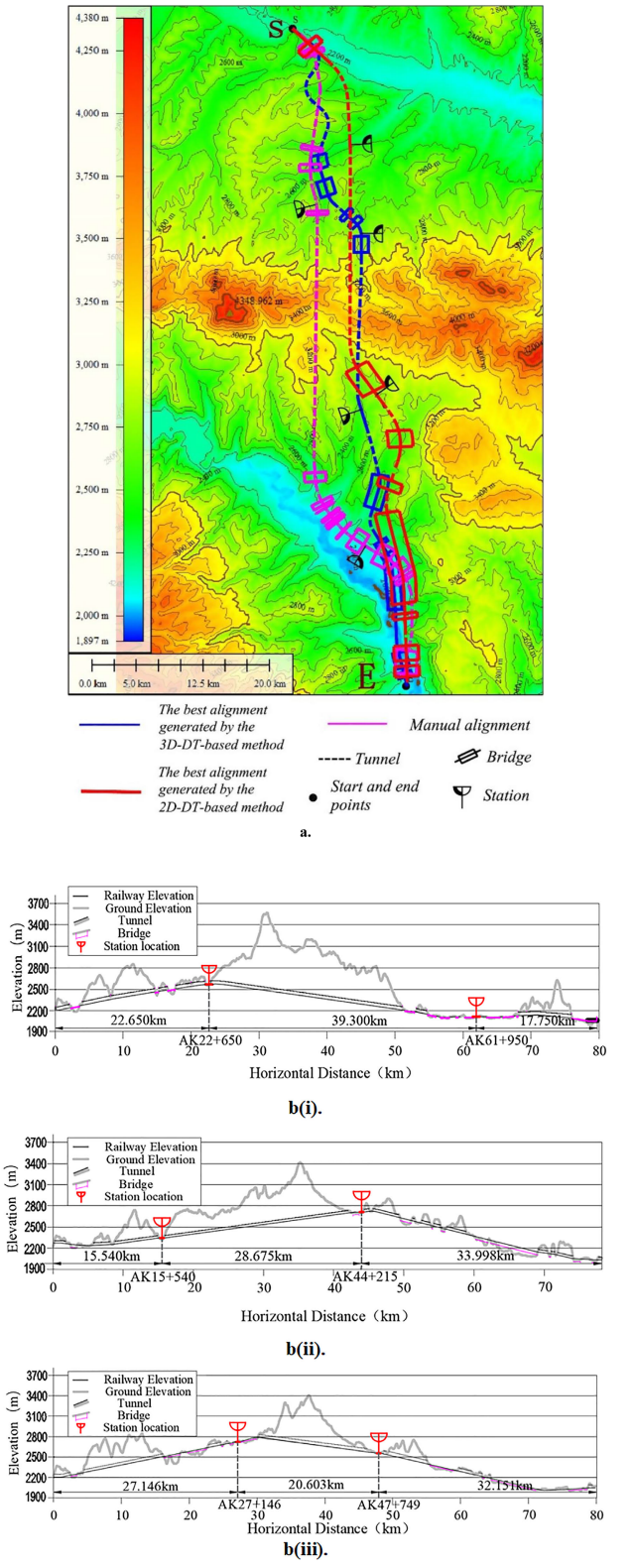

FIGURE 19. (a) Comparison of manually designed and computer-generated horizontal alternatives. (b) Comparison of manually designed and computer-generated vertical alternatives: b(i). Manual alternative; b(ii). The lowest-cost alternative generated with the 2DDT-based method; b(iii). The lowest-cost alternative generated with the proposed 3DDT-based method.

optimization method can generate a number of feasible alternatives while the solutions' qualities are also enhanced.

The above results confirm that this approach can offer a greater variety of promising alternatives with higher qualities, while handling the complex coupling constraints. These alternatives offer valuable options and can be considered by designers when evaluating and improving their alternatives.

V. CONCLUSION

The design of railway alignments and station locations is a complex and time-consuming engineering problem. Especially in mountainous regions, the large 3D search spaces, infinite numbers of potential alternatives, complex and coupling constraints of this problem pose many challenges. This paper proposes a new concurrent railway alignment and station location optimization method for mountainous areas based on the 3-dimensional distance transform algorithm (3DDT, [25]). The effectiveness and practicability of the algorithm are verified through a real-world case study in a complex mountainous area. The main improvements provided by this method can be summarized as follows:

(1) A 3-dimensional optimization model for concurrently optimizing railway alignment and station locations is developed, considering coupling constraints and using construction and operation costs as the objective function. Additionally, the feasible 3D search spaces for alignment and stations are greatly enlarged by using the developed 3D-DT algorithm.

(2) A total of four neighboring masks are employed in the developed 3D-DT algorithm. Besides the basic alignment 3D search neighboring mask, the combined-alignment-station 3D search neighboring mask is constructed to search for both alignment and stations as well as to handle the constraints of maximum gradient and flat area of the station. Moreover, two reverse perceptual neighboring masks are also proposed to find the potential link paths in subsequent searches.

(3) A 3DDT-based search algorithm incorporating a perceptual search strategy is proposed to find the potential link paths in subsequent searches and determine the best station location within the specific spacing interval. This search algorithm is able to search for both alignment and the stations during the optimization process and find the optimized combination schemes, without ignoring the coupling constraints or limiting the search space.

(4) This method has been applied to a real-world problem in a complex mountain area. The 3DDT-based concurrent optimization method can generate a number of feasible alternatives while the solutions' qualities are also enhanced. The lowest-cost alternative generated with the proposed method costs 13.23% less than a manual alternative designed by experienced designers and 7.16% less than the lowest-cost alternative generated with the 2DDT-based method.

This paper mainly solves the problem of optimizing the railway alignment and station locations concurrently in complex mountainous areas while considering the coupling constraints among them. However, geologic hazards such as landslides and debris flows, and the effects of regional populations and economic status, which are not considered here, may also be decisive factors for alignment and stations design in mountainous regions. Thus, future work may account for such factors in seeking better solutions. Besides, it may also be useful to extend the current optimization model to a multi-objective optimization model involving construction and operation costs, resulting demand, environmental impacts and other objectives, in order to further explore the tradeoffs among various factors.

REFERENCES

[1] A. M. Wellington, *The Economic Theory of the Location of Railways*. New York, NY, USA: Wiley, 1877, pp. 15–64.
[2] J. F. B. Shaw and B. E. Howard, "Comparison of two integration methods in transportation routing," *Transp. Res. Rec.*, vol. 806, pp. 8–13, Jan. 1981. [Online]. Available: http://worldcat.org/isbn/0309032202
[3] F. Y. M. Wan, *Introduction to the Calculus of Variations and its Applications*. New York, NY, USA: Chapman & Hall, 1995, pp. 115–121.
[4] R. Robinson, "Automatic design of the road vertical alignment," in *Proc. PTRC Seminar Cost Models Optim. Highways (Session L19)*, Washington, DC, USA, 1973, pp. 24–56.
[5] E. P. Chew, C. J. Goh, and T. F. Fwa, "Simultaneous optimization of horizontal and vertical alignments for highways," *Transp. Res. B, Methodol.*, vol. 23, no. 5, pp. 315–329, Oct. 1989, doi: 10.1016/0191-2615(89)90008-8.
[6] C. S. Revelle, E. Whitlach, and J. Wright, *Civil and Environmental Systems Engineering*. Upper Saddle River, NJ, USA: Prentice-Hall, 1996, p. 507.
[7] S. M. Easa, "Selection of roadway grades that minimize Earthwork cost using linear programming," *Transp. Res. A, Gen.*, vol. 22, no. 2, pp. 121–136, Jan. 1988, doi: 10.1016/0191-2607(88)90024-6.
[8] Y. Shafahi and M. Bagherian, "A customized particle swarm method to solve highway alignment optimization problem," *Comput.-Aided Civil Infrastruct. Eng.*, vol. 28, no. 1, pp. 52–67, Jan. 2013, doi: 10.1111/j.1467-8667.2012.00769.x.
[9] H. Pu, T. Song, P. Schonfeld, W. Li, H. Zhang, J. Hu, X. Peng, and J. Wang, "Mountain railway alignment optimization using stepwise & hybrid particle swarm optimization incorporating genetic operators," *Appl. Soft Comput.*, vol. 78, pp. 41–57, May 2019, doi: 10.1016/j.asoc.2019.01.051.
[10] H. Zhang, H. Pu, P. Schonfeld, T. Song, and W. Li, "Multi-objective railway alignment optimization considering costs and environmental impacts," *Appl. Soft Comput.*, vol. 89, Apr. 2020, Art. no. 106105, doi: 10.1016/j.asoc.2020.106105.
[11] J. C. Jong, "Optimizing highway alignments with genetic algorithms," Ph.D. dissertation, Dept. Civ. Eng., Univ. Maryland, College Park, MD, USA, 1998.
[12] J. C. Jong and P. Schonfeld, "An evolutionary model for simultaneously optimizing three-dimensional highway alignments," *Transp. Res. B, Methodol.*, vol. 37, no. 2, pp. 107–128, Feb. 2003, doi: 10.1016/S0191-2615(01)00047-9.
[13] M. K. Jha and P. Schonfeld, "A highway alignment optimization model using geographic information systems," *Transp. Res. A: Policy Pract.*, vol. 38, no. 6, pp. 455–481, Jul. 2004, doi: 10.1016/j.tra.2004.04.001.
[14] S. Samanta and M. K. Jha, "Identifying feasible locations for rail transit stations: Two-stage analytical model," *Transp. Res. Rec.*, vol. 45, no. 1, pp. 31–45, Jan. 2011, doi: 10.3141/2063-10.
[15] X. Lai and P. Schonfeld, "Concurrent optimization of rail transit alignments and station locations," *Urban Rail Transit*, vol. 2, no. 1, pp. 1–15, Mar. 2016, doi: 10.1007/s40864-016-0033-1.
[16] G. C. Athanassoulis and V. Calogero, "Optimal location of a new highway from A to BA computer technique for route planning," in *Proc. PTRC Seminar Cost Models Optim. Highways (Session L19)*, Washington, DC, USA, 1973, p. 9.
[17] J. D. Hogan, "Experience with OPTLOC: Optimum location of highway by computer," in *Proc. PTRC Seminar Cost Models Optim. Highways (Session L10)*, Washington, DC, USA, 1973, pp. 78–92.

[18] T. F. Fwa, "Highway vertical alignment analysis by dynamic programming," *Transp. Res. Rec.*, vol. 1239, nos. 1–9, pp. 2–3, 1989. [Online]. Available: http://onlinepubs.trb.org/Onlinepubs/trr/1989/1239/1239-001.pdf

[19] S. M. Easa and A. Mehmood, "Optimizing design of highway horizontal alignments: New substantive safety approach," *Comput.-Aided Civil Infrastruct. Eng.*, vol. 23, no. 7, pp. 560–573, Oct. 2008, doi: 10.1111/j.1467-8667.2008.00560.x.

[20] Y. Pushak, W. Hare, and Y. Lucet, "Multiple-path selection for new highway alignments using discrete algorithms," *Eur. J. Oper. Res.*, vol. 248, no. 2, pp. 415–427, Jan. 2016, doi: 10.1016/j.ejor.2015.07.039.

[21] M. J. de Smith, "Determination of gradient and curvature constrained optimal paths," *Comput.-Aided Civil Infrastruct. Eng.*, vol. 21, no. 1, pp. 24–38, Jan. 2006, doi: 10.1111/j.1467-8667.2005.00414.x.

[22] W. Li, H. Pu, P. Schonfeld, H. Zhang, and X. Zheng, "Methodology for optimizing constrained 3-dimensional railway alignments in mountainous terrain," *Transp. Res. C, Emerg. Technol.*, vol. 68, pp. 549–565, Jul. 2016, doi: 10.1016/j.trc.2016.05.010.

[23] W. Li, H. Pu, P. Schonfeld, J. Yang, H. Zhang, L. Wang, and J. Xiong, "Mountain railway alignment optimization with bidirectional distance transform and genetic algorithm," *Comput.-Aided Civil Infrastruct. Eng.*, vol. 32, no. 8, pp. 691–709, Jun. 2017, doi: 10.1111/mice.12280.

[24] H. Pu, H. Zhang, W. Li, J. Xiong, J. Hu, and J. Wang, "Concurrent optimization of mountain railway alignment and station locations using a distance transform algorithm," *Comput. Ind. Eng.*, vol. 127, pp. 1297–1314, Jan. 2019, doi: 10.1016/j.cie.2018.01.004.

[25] H. Pu, T. Song, P. Schonfeld, W. Li, H. Zhang, J. Wang, and X. Peng, "A three-dimensional distance transform for optimizing constrained mountain railway alignments," *Comput.-Aided Civil Infrastruct. Eng.*, vol. 34, no. 11, pp. 972–990, Jun. 2017, doi: 10.1111/mice.12475.

[26] T. Song, H. Pu, P. Schonfeld, W. Li, and X. Peng, "Parallel Three-dimensional distance transform for railway alignment optimization using openMP," *J. Transp. Eng., A, Syst.*, vol. 146, no. 5, pp. 2473–2907, May 2020, doi: 10.1061/JTEPBS.0000344.

[27] A. Rosenfeld and J. L. Pfaltz, "Sequential operations in digital picture processing," *J. ACM*, vol. 13, no. 4, pp. 471–494, Oct. 1966, doi: 10.1145/321356.321357.

[28] V. R. Vuchic and G. F. Newell, "Rapid transit interstation spacings for minimum travel time," *Transp. Sci.*, vol. 2, no. 4, pp. 303–339, Nov. 1968, doi: 10.1287/trsc.2.4.303.

[29] V. R. Vuchic, "Rapid transit interstation spacings for maximum number of passengers," *Transp. Sci.*, vol. 3, no. 3, pp. 214–232, Aug. 1969, doi: 10.1287/trsc.3.3.214.

[30] S. C. Wirasinghe, V. F. Hurdle, and G. F. Newell, "Optimal parameters for a coordinated rail and bus transit system," *Transp. Sci.*, vol. 11, no. 4, pp. 359–374, Nov. 1977, doi: 10.1287/trsc.11.4.359.

[31] S. C. Wirasinghe, "Nearly optimal parameters for a rail/feeder-bus system on a rectangular grid," *Transp. Res. A, Gen.*, vol. 14, no. 1, pp. 33–40, Feb. 1980, doi: 10.1016/0191-2607(80)90092-8.

[32] S. Chien and P. Schonfeld, "Joint optimization of a rail transit line and its feeder bus system," *J. Adv. Transp.*, vol. 32, no. 3, pp. 253–284, Jun. 1998, doi: 10.1002/atr.5670320302.

[33] G. Laporte, J. A. Mesa, and F. A. Ortega, "Locating stations on rapid transit lines," *Comput. Oper. Res.*, vol. 29, no. 6, pp. 741–759, Dec. 2002, doi: 10.1016/S0305-0548(00)00013-7.

[34] G. Laporte, J. A. Mesa, F. A. Ortega, and F. Perea, "Planning rapid transit networks," *Socio-Econ. Planning Sci.*, vol. 45, no. 3, pp. 95–104, Sep. 2011, doi: 10.1016/j.seps.2011.02.001.

[35] J. M. Gleason, "A set covering approach to bus stop location," *Omega*, vol. 3, no. 5, pp. 605–608, Oct. 1975, doi: 10.1016/0305-0483(75)90033-X.

[36] A. T. Murray, "Strategic analysis of public transport coverage," *Socio-Econ. Planning Sci.*, vol. 35, no. 3, pp. 175–188, Sep. 2001, doi: 10.1016/S0038-0121(01)00004-0.

[37] A. T. Murray, "A coverage model for improving public transit system accessibility and expanding access," *Ann. Oper. Res.*, vol. 123, nos. 1–4, pp. 143–156, Oct. 2003, doi: 10.1023/A:1026123329433.

[38] C. Wu and A. T. Murray, "Optimizing public transit quality and system access: The multiple-route, maximal Covering/Shortest-path problem," *Environ. Planning B: Planning Des.*, vol. 32, no. 2, pp. 163–178, Apr. 2005, doi: 10.1068/b31104.

[39] H. W. Hamacher, A. Liebers, A. Schbel, D. Wagner, and F. Wagner, "Locating new stops in a railway network," *Electron. Notes Theor. Comput. Sci.*, vol. 50, no. 1, pp. 13–23, Aug. 2001, doi: 10.1016/S1571-0661(04)00162-8.

[40] A. Schöbel, "Locating stops along bus or railway lines—A bicriteria problem," *Ann. Oper. Res.*, vol. 136, no. 1, pp. 211–227, Apr. 2005, doi: 10.1007/s10479-005-2046-0.

[41] A. SCHöBEL, H. W. Hamacher, A. Liebers, and D. Wagner, "The continuous stop location problem in public transportation networks," *Asia–Pacific J. Oper. Res.*, vol. 26, no. 1, pp. 13–30, Feb. 2009, doi: 10.1142/S0217595909002080.

[42] E. Kranakis, P. Penna, K. Schlude, and D. S. Taylor, "Improving customer proximity to railway stations," in *Proc. 5th Italian Conf. Algorithms Complex.*, Berlin, Germany, 2003, pp. 264–276.

[43] D. R. P. Groß, H. W. Hamacher, S. Horn, and A. Schöbel, "Stop location design in public transportation networks: Covering and accessibility objectives," *TOP*, vol. 17, no. 2, pp. 335–346, Dec. 2009, doi: 10.1007/s11750-008-0061-4.

[44] A. H. Lovett, G. Munden, M. R. Saat, and C. P. L. Barkan, "High-speed rail network design and station location: Model and sensitivity analysis," *Transp. Res. Rec.*, vol. 2374, no. 1, pp. 1–8, Jan. 2013, doi: 10.3141/2374-01.

[45] J. R. Current, C. S. R. Velle, and J. L. Cohon, "The maximum covering/shortest path problem: A multiobjective network design and routing formulation," *Eur. J. Oper. Res.*, vol. 21, no. 2, pp. 189–199, Aug. 1985, doi: 10.1016/0377-2217(85)90030-X.

[46] H. Dufourd, M. Gendreau, and G. Laporte, "Locating a transit line using tabu search," *Location Sci.*, vol. 4, nos. 1–2, pp. 1–19, May/Aug. 1996, doi: 10.1016/S0966-8349(96)00008-3.

[47] G. Bruno, M. Gendreau, and G. Laporte, "A heuristic for the location of a rapid transit line," *Comput. Oper. Res.*, vol. 29, no. 1, pp. 1–12, Jan. 2002, doi: 10.1016/S0305-0548(00)00051-4.

[48] H. Pu, L. Zhao, W. Li, J. Zhang, Z. Zhang, J. Liang, and T. Song, "A global iterations method for recreating railway vertical alignment considering multiple constraints," *IEEE Access*, vol. 7, pp. 121199–121211, Aug. 2019, doi: 10.1109/ACCESS.2019.2937658.

HAO PU was born in Nanchong, Sichuan, China, in May 1973. He received the B.S., M.S., and Ph.D. degrees from Central South University, Hunan, in 1994, 1997, and 2002, respectively.

In 1994, he joined Central South University, where he is currently a Professor with the Railway Engineering Department, School of Civil Engineering. He has authored four books, and more than 50 articles and six inventions. His research interests include computer-aided design of road & railway, network-based three-dimensional simulation and visualization, virtual reality, road & railway alignment optimization, station locations optimization, and the network-based visualization for operation and management of mechanical and electrical equipment.

Dr. Pu is the Chairman of the Digital Construction Department, National Engineering Laboratory for High Speed Railway Construction Technology, and also the Vice Chairman of the Alignment Department, China Railway Society.

XIAOMING LI was born in Hohhot, Inner Mongolia, China, in 1995. He received the B.E. degree in civil engineering from Central South University, Changsha, in 2018, where he is currently pursuing the M.S. degree in railway engineering with the School of Civil Engineering.

His research interests include railway alignment and station locations optimization.

PAUL M. SCHONFELD received the B.S. and M.S. degrees in civil engineering from the Massachusetts Institute of Technology, in 1974, and the Ph.D. degree in civil engineering from the University of California at Berkeley, Berkeley, in 1978.

From 1972 to 1973, he was a Teaching Assistant with the Massachusetts Institute of Technology. From 1975 to 1977, he was a Research Assistant with the University of California at Berkeley. From 1978 to 1984, he was an Assistant Professor of civil engineering with the University of Maryland at College Park, College Park, where he was an Associate Professor from 1984 to 1993 and he has been a Professor with the Department of Civil and Environment Engineering, since 1993. He has hosted several U.S. Natural Science Foundation projects and published more than 480 articles. More than 20 Ph.D. students have been awarded tenure.

Dr. Paul has been a Fellow of the American Society of Civil Engineers (ASCE), since 1994. He received the ASCE's 2018 James Laurie Prize for Transportation Engineering Professional Achievement. He served *Journal Editors* and the Deputy Editor for *Advanced Transportation* and *Journal of Transportation Engineering, Part A: Systems* (ASCE).

WEI LI was born in Nanchang, Jiangxi, China, in July 1984. He received the B.S. degree in civil engineering from Central South University (CSU), China, in 2006, and the M.S. and Ph.D. degrees in road and rail engineering from CSU, in 2009.

He is currently an Associate Professor with the Railway Engineering Department, School of Civil & Architecture, Central South University. He has published more than 20 articles in journals and international refereed conferences. His research interests include the computer-aided design of road & railway, optimization of road & railway alignment, building information modeling, network-based three-dimensional simulation and visualization, and virtual reality and network-based visualization for operation and management of mechanical and electrical equipment.

JIAN ZHANG (Member, IEEE) received the B.E. degree in computer science from the National University of Defense Technology, in 1998, and the M.E. and Ph.D. degrees in computer science from Central South University, in 2002 and 2007, respectively.

He is currently an Associate Professor with the School of Computer Science and Engineering, Central South University. He has published more than 30 articles in journals and international refereed conferences. His research interests include optimization theory, cyberspace security, cloud computing, and cognitive radio technology.

Dr. Zhang is a Fellow of the Association for Computing Machinery (ACM) and China Computer Federation (CCF).

JIE WANG was born in Shaodong, Hunan, China, in 1974. He received the B.E. degree in civil engineering from Central South University, Changsha, in 1998.

Since 1998, he has been an Engineer of the Division of Railway Transportation, China Railway First Survey and Design Institute Group Company, Ltd., where he is currently a Professorate Senior Engineer and the Deputy Chief Engineer. He has authored 15 articles and more than 10 inventions. His research interests include the optimization and design of railway station, computer-aided design of road & railway, the optimization of railway alignment, and the planning of intercity railway network in urban agglomeration.

JIANPING HU was born in Shaoyang, Hunan, China, in 1971. He received the B.E. degree in civil engineering from Central South University, Changsha, in 1994, and the M.S. degree in architecture and civil engineering from Southwest Jiaotong University, Chengdu, in 2011.

Since 1994, he has been an Engineer with China Railway Eryuan Engineering Group Company, Ltd., Chengdu, where he is currently a Professorate Senior Engineer. He has authored 20 articles. His research interests include project management, railway alignment intelligent optimization, and the computer-aided design of railway alignment and stations.

XIANBAO PENG was born in Guangshui, Hubei, China, in 1968. He received the B.E. degree in civil engineering and the M.S. degree in architecture and civil engineering from Central South University, Changsha, in 1992 and 1992, respectively.

Since 1992, he has been an Engineer with China Railway Siyuan Survey and Design Group Company, Ltd., Hubei, where he is currently a Professorate Senior Engineer. He has authored 17 articles. His research interests include railway alignment survey and design methods, BIM technology for railway design, the intelligent optimization of alignment and stations, and reconstruction and expansion of existing railway alignment.